



Design and Simulation of a semi-transparent photovoltaic thermal (PVT) indirect solar dryer integrated with kitchen chimney using ANN technique

Prashant Bhardwaj^{a*}, Sujata Nayak^a, Arvind Tiwari^b, & G N Tiwari^b

^aDepartment of Mechanical Engineering, Manav Rachna University, Faridabad, Haryana 121 004 India

^bBag Energy Research Society, Jawahar Nagar (Margapur), Chilkhar, Ballia 221 701, India

Received: 1 February 2021; Accepted: 25 August 2021

In the proposed research, an effort has been made to develop a thermal model for a semi-transparent PVT solar dryer integrated with a kitchen chimney for faster drying of agricultural produce to enhance their shelf life. The thermal model is based on energy balance equations derived based on the design of the dryer and different climatic parameters for April month in New Delhi. It has been observed that there is an increase of 8°C in the drying chamber for the initial kitchen chimney outlet temperature of 72°C with a packing factor of 0.83 for the semi-transparent solar cells, which has also been validated by the ANN model. An exhaust fan placed between the PVT air collector and drying chamber is operated using electrical energy generated from the PVT air collector, making the entire set up self-sustainable.

Keywords: Photovoltaic-thermal, ANN Technique, Energy, Exergy

1 Introduction

Drying is an important method for the preservation of fruits and vegetables which helps in increase their shelf life as well as transportation. The drying process, when used properly, maintains the nutrient quality of food, requires minimal effort and reduces post-harvest loss significantly. Collector efficiency of an indirect solar dryer having a North-South reflector with natural convection drying process is enhanced without load by 18.5% from 40.0% to 58.5% even in January, the corresponding heat transfer values are 36.5% to 50.3% respectively¹. Solar dryer with forced convection in which drying chamber is connected with double pass V-corrugated solar heater is developed. The drying process is performed with Thymus and mint which are at a temperature of 29°C initially. It has been observed that for drying of Thymus with the moisture content of 95% initially, it took 34 hours to reach a final moisture content of 11±0.5% and in the case of mint with the moisture content of 85% initially, it took 5 hours to reach a final moisture content of 11 ± 0.5% in 39°C to 54°C². Indirect solar drying method for banana drying with an efficiency of 22% consists of solar flat plate air collector with V-corrugated absorber and insulated

drying chamber developed³. A new concept of an indirect solar dryer in which solar air collector is consists of two fixed corrugated aluminum forming a parallel cylinder which allows the air to circulate along with the collector. It has been found that the average thermal efficiency of this drying chamber is 11.11%⁴. In a new method, to design an indirect solar dryer in forced convection mode Phase Change Material (PCM) is also used. It maintains the drying chamber temperature to 4 to 16°C higher than the ambient temperature⁵. A system design analysis for solar drying of Stevia leaves, a system design analysis is done using direct and indirect solar drying technology based on Weibull model showed that indirect solar drying is having the better superior condition, drying times, operating conditions control. Also, it has greater protection against the effects of temperature⁶. A hybrid PVT greenhouse dryer designed with a DC fan for forced convection The results showed the prediction for moisture evaporation with natural convection is better than with forced convection⁷. To predict the performance of a PVT greenhouse collector, a thermal model for energy and exergy is developed and analyzed to predict its performance. From experimental results, it is observed that solar cell temperature is 3°C to 4°C more than the temperature of tedlar back surface and 15°C to 16°C more than the green-house room air

*Corresponding author (E-mail: prashant@mru.edu.in)

temperature. It is also found that exergy efficiency for PVT integrated greenhouse is 4%⁸. A simple mathematical model is developed for PVT and earth air heat exchanger (EAHE) which is integrated with the greenhouse to study its effectiveness for a year. It is found from the results that in the winter season the temperature is increased by 7°C to 8°C inside the greenhouse where at night the PVT is coupled with EAHE, considered to be suitable for plant growth during winter period⁹. The performance of a space heater which consists of a hybrid PVT double pass facade has been studied. It is found from the results that for space heating in a building, the double pass air facade is most useful on a typical winter day as it increases the room air temperature by 5°C to 6°C¹⁰. Exergo-economic analysis for a hybrid PVT air collector concluded that it can be used to save energy and has more potential as compared to PV module thus it is relatively very useful for space heating in cold areas and to dry medicinal plants¹¹. The overall exergy efficiency of a glazed hybrid single channel photovoltaic thermal module is optimized using Genetic Algorithm (GA) and Genetic Algorithm - Fuzzy System (GA-FS) and it is found that the overall exergy efficiency obtained from the system optimized with GA-FS is 1.27% higher than the efficiency obtained from the system optimized with GA and 5.4% higher than the efficiency obtained from the un-optimized system.^{12,13} Single channel photovoltaic thermal module is again optimized for overall exergy gain and overall thermal gain with an Evolutionary Algorithm (EA). It has been observed that annual overall exergy gain and annual overall thermal gain has been increased by 69.52% and 88.05% respectively than the un-optimized system.¹⁴ Energy and exergy analysis of a hybrid greenhouse dryer of different photovoltaic modules at different weather conditions has been studied. From the results, it was found that the C-Si type PV module is most efficient because of the module productivity and expected life¹⁵. An experiment on solar hybrid dryer for pineapple drying observed that drying time is very much less and food quality is found to be better in the case of hybrid dryer¹⁶. Performance analysis of photovoltaic thermal mixed-mode greenhouse dryer is carried out by considering different parameters. It is concluded that the quality of the product is increased and de-colouration is also minimized¹⁷. Performance analysis of a solar-heat recovery assisted infrared dryer has been studied for drying of melon and it is

found that the efficiency of the dryer can be enhanced by using a heat exchanger which converts waste energy from the dryer chimney to heat the inlet air by using heat recovery¹⁸. A solar dryer in which waste heat energy from a split AC external unit is used to enhance the drying rate increased efficiency by about 13%¹⁹.

In this paper, a semi-transparent PVT solar dryer which is integrated with the kitchen chimney has been analyzed and simulated for four different kitchen chimney exhaust air temperatures. Energy and Exergy analysis of the proposed model has been done & the same is validated with the ANN model.

2 Materials and Methods

An indirect type solar dryer has been designed which consists of a semi-transparent PVT air collector unit and a chamber for drying purpose. The collector unit consists of flat blackened absorber plate in which a rectangular shaped duct is attached. The collector unit is integrated with the outlet of the kitchen chimney which consists of a semi-transparent PV module and a flat plate collector. The air entering into the collector unit is preheated by solar radiation received at non-packing factor area below the semi-transparent PV module by the absorber. Hot air from the kitchen chimney forces itself towards the drying chamber unit via the semi-transparent PVT air collector and gets further heated by the heat trapped by the absorber unit. This hot air absorbs moisture from the food which is kept on wire mesh trays for drying while flowing in an upward direction in the drying chamber. At top of the drying chamber in the east and west walls two exhausts are provided. Duct dimensions are 2.2m x 0.65m x 0.05m and 50W semi-transparent PV module is attached on it. PVT collector unit is kept at an angle of 30° with the horizontal to receive maximum amount of solar radiation. The schematic diagram of the hybrid dryer integrated with the Kitchen Chimney is presented in Fig. 1. Intensity of solar radiation and ambient temperature values concerning time have been taken for the analysis under no-load conditions. Analysis of dryer is carried out for four different chimney outlet temperatures i.e. T_{ch1} is 37°C, T_{ch2} is 47°C, T_{ch3} is 57°C and T_{ch4} is 72°C (whose values are assumed to be greater than the ambient temperature). Using thermal modeling equations, the following parameters have been calculated hourly:

- a) Outlet temperature
- b) Solar cell temperature

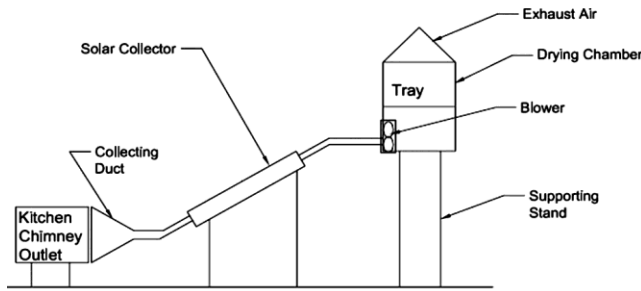


Fig. 1 — Schematic diagram of indirect semi-transparent PVT solar dryer integrated with kitchen chimney.

- c) Thermal energy
- d) Electrical energy
- e) Exergy
- f) Thermal efficiency
- g) Electrical efficiency

2.2 THERMAL modelling of indirect type PVT dryer

Energy balance equations are written for the thermal modelling of the proposed semi-transparent type indirect PVT dryer by considering the following assumptions:

- i) Quasi-steady state condition has been considered for the proposed system.
- ii) Absorptivity is neglected for enclosed air between glasses of semi-transparent PV module.
- iii) The transmissivity is considered as 100% for Ethyl Vinyl Acetate.
- iv) The temperature variation is neglected along with the thickness and width.
- v) Resistance losses of solar cell have been neglected.

Using 1st law of thermodynamics, energy balance equations for the proposed dryer have been written as:

2.2.1 For semitransparent PV module

The energy balance equation for semitransparent PV module solar cells can be written as²⁰,

$$\alpha_c \tau_g \beta_c I(t) b dx = [U_{tc,a}(T_c - T_a) + U_{tc,f}(T_c - T_f) b dx + \tau_g \eta_c \alpha_c \beta_c I(t) b dx] \quad \dots (1)$$

where, α_c is the absorptivity of solar cell,
 τ_g is the transmissivity of glass,
 $I(t)$ is the incident solar intensity in W/m^2 ,
 $U_{tc,a}$ is the overall heat transfer coefficient from solar cell to ambient in $W/m^2 \text{ } ^\circ C$,
 T_c is the solar cell Temperature in $^\circ C$
 T_a is the ambient temperature in $^\circ C$,
 T_f is the flowing air temperature in $^\circ C$,

b is the width in m, and,
 η_c is the efficiency of solar cell
 Solving for solar cell temperature, one gets

$$T_c = \frac{\tau_g \alpha_c \beta_c (1 - \eta_c) I(t) + U_{tc,a} T_a + U_{tc,f} T_f}{U_{tc,a} + U_{tc,f}} \quad \dots (2)$$

2.2.2 For blackened absorber plate

The energy balance equation for absorber plate is given by,

$$[\alpha_p (1 - \beta_c) \tau_g^2 I(t)] b dx = [h_{p,f}(T_p - T_f) + U_{bp,a}(T_p - T_a)] b dx \quad \dots (3)$$

where, α_p is the transmissivity of absorber plate,
 T_p is the absorber plate temperature in $^\circ C$,
 $h_{p,f}$ is the heat transfer coefficient between absorber plate and flowing air in $W/m^2 \text{ } ^\circ C$, and,
 $U_{bp,a}$ is the overall back loss coefficient from flowing air to ambient in $W/m^2 \text{ } ^\circ C$

After solving for absorber plate temperature, one has the expression for (T_p),

$$T_p = \frac{\alpha_p (1 - \beta_c) \tau_g^2 I(t) + h_{p,f} T_f + U_{bp,a} T_a}{U_{bp,a} + h_{p,f}} \quad \dots (4)$$

2.2.3 For the air flowing through the duct

The energy balance equation for the air which is flowing through the absorber plate is,

$$\dot{m}_a C_a \frac{dT_f}{dx} dx = [h_{p,f}(T_p - T_f) + U_{tc,f}(T_c - T_f)] b dx \quad \dots (5)$$

where, \dot{m}_a is the rate of flow of air in kg/s,
 $U_{tc,f}$ is the overall heat transfer coefficient from solar cell to flowing air in $W/m^2 \text{ } ^\circ C$, and,
 C_a is the specific heat in $J/kg \text{ } ^\circ C$

For the boundary condition, $x=0$, $T_f=T_{ch}$ and at $x=L$, $T_f=T_{fo}$, Eq(5) can give the following expression

$$T_{fo} = \left[\frac{(\alpha \tau)_{m,eff} I(t)}{U_{L,m}} + T_a \right] \left[1 - \exp\left(-\frac{b U_{L,m} L}{\dot{m}_a C_a}\right) \right] + T_{ch} \left[\exp\left(-\frac{b U_{L,m} L}{\dot{m}_a C_a}\right) \right] \quad \dots (6)$$

where, $(\alpha \tau)_{m,eff}$ is the product of effective absorptivity and transmissivity of PV module

T_{fo} is the outgoing flowing air temperature in $^\circ C$,
 T_{ch} is the kitchen chimney outlet temperature in $^\circ C$,
 L is the length in m, and,
 $U_{L,m}$ is the overall heat transfer coefficient in $W/m^2 \text{ } ^\circ C$

At the end of the semi-transparent PVT collector, the rate of thermal energy available can be evaluated as,

$$\dot{Q}_{u,m} = \dot{m}_a C_a (T_{fo} - T_{ch}) \quad \dots (7)$$

Using Eq(6) and Eq(7), we get

$$\dot{Q}_{u,m} = A_m F_{Rm} [(\alpha\tau)_{m,eff} I(t) - U_{L,m} (T_{ch} - T_a)] \quad \dots (8)$$

where, A_m is the Area of module in m^2 , and, F_{Rm} is the heat removal factor

2.2.4 Instantaneous thermal efficiency

An instantaneous thermal efficiency for semi-transparent PVT collector can be evaluated by,

$$\eta_i = \frac{\dot{Q}_u}{N_{cl} \times A_c \times I(t)} \quad \dots (9)$$

where, N_{cl} is the number of clear hours in a day

2.2.4 Electrical efficiency

After knowing T_c from Eq. (2), using Eq. (4) & Eq. (6), Electrical efficiency can be obtained as

$$\eta_{el} = \eta_o [1 - 0.0045(T_c - 25)] \quad \dots (10)$$

where, η_o is the efficiency at standard condition at $I(t) = 1000W/m^2$ and $T_a = 25^\circ C$

2.2.5 Electrical energy

The hourly electrical energy produced by the solar panel can be obtained by

$$E_{el} = \frac{\eta_{el} \times I(t) \times A_m \times N_{cl}}{1000} \quad \dots (11)$$

2.2.6 Energy gain

Energy analysis can be made and the overall thermal gain is evaluated as

$$\sum \dot{Q}_{u,overall} = \sum \dot{Q}_{u,th} + \frac{\sum \dot{Q}_{u,el}}{\zeta - power} \quad \dots (12)$$

The electrical energy is divided by electric power generation efficiency (ζ) to convert it from a high-grade form of energy to a low-grade form of energy as equivalent to the thermal energy²¹.

2.2.7 Exergy gain

Exergy analysis can be made by using second law of thermodynamics and total exergy-in, exergy-out, and exergy destructured from the system can be evaluated as²²

$$\sum \dot{E}x_{in} - \sum \dot{E}x_{out} = \sum \dot{E}x_{dest} \quad \dots (13)$$

Or

$$\sum \dot{E}x_{in} - \sum (\dot{E}x_{th} + \dot{E}x_{el}) = \sum \dot{E}x_{dest} \quad \dots (14)$$

where, $\dot{E}x_{th}$ is the thermal exergy in KWh, and,

$\dot{E}x_{el}$ is the electrical exergy in KWh

where,

$$\begin{aligned} \dot{E}x_{in} &= A_c \times N_{cl} \times I(t) \times \left[1 - \frac{4}{3} \times \left(\frac{T_a}{T_s} \right) + \frac{1}{3} \times \left(\frac{T_a}{T_s} \right)^4 \right] \quad \dots (15) \end{aligned}$$

$$\begin{aligned} \dot{E}x_{th} &= \dot{m}_a c_a \left[(T_{fo} - T_{ch}) - (T_a + 273) \ln \frac{T_{fo} + 273}{T_{ch} + 273} \right] \quad \dots (16) \end{aligned}$$

$$\dot{E}x_{el} = \eta_{el} \times A_m \times I(t) \quad \dots (17)$$

$$\dot{E}x_{out} = \dot{E}x_{th} + \dot{E}x_{el} \quad \dots (18)$$

2.2.8 Software description

MATLAB R2018a has been used for the calculation of solar cell temperature, absorber temperature, and outletduct air temperature. Artificial Neural Network (ANN) technique is used to validate the results of energy and exergy analysis. Artificial Neural Network Toolbox of MATLAB R2018a from the two-layer feed-forward network with 10 neurons in the hidden layer and Levenberg-Marquardt algorithm with hyperbolic tangent sigmoid transfer function. In this paper, data is used to trained, validated and tested to develop an ANN structure which is shown in Fig. 2. Variation of values of solar intensity, ambient temperature and kitchen chimney outlet temperature with time has been used as input parameters for New Delhi climatic conditions in April 2018. The temperature of the solar cell, absorber plate & outlet air, thermal energy, thermal efficiency, electrical energy, electrical efficiency and exergy has been considered as the output parameters.

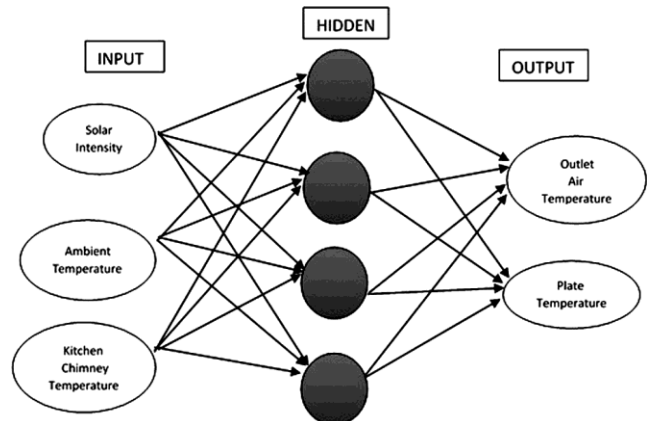


Fig. 2 — Selected ANN structure for the proposed setup.

3 Results and Discussion

Equations (2, 4, and 6) have been computed using MATLAB software for a proposed design parameters which is given in Table 1 and the value of solar intensity and ambient temperature variation on an

Table 1 — Design Parameter values for the proposed semi-transparent PVT Dryer

Design Parameters	Values
A_c	1.07m ²
A_m	0.357m ²
C_a	1005J/kgK
F_{Rm}	1.0
$h_{p,f}$	14.82W/m ² K
\dot{m}	0.078kg/s
$U_{bp,a}$	0.68 W/m ² K
U_{Lm}	3.58 W/m ² K
$U_{tc,a}$	9.5 W/m ² K
$U_{tc,f}$	5.7 W/m ² K
α_c	0.9
β_c	0.83
η_o	0.12
α_p	0.8
τ_g	0.95

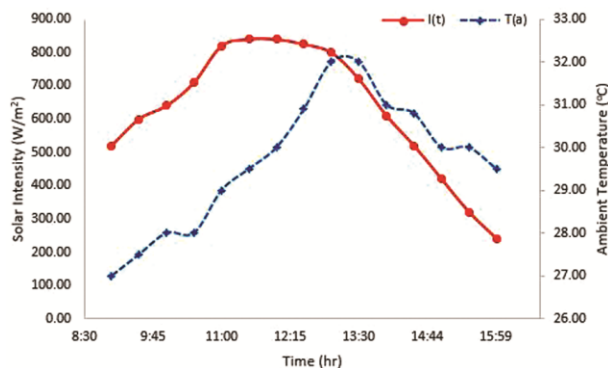


Fig. 3 — Solar intensity and ambient temperature variation on an hourly basis.

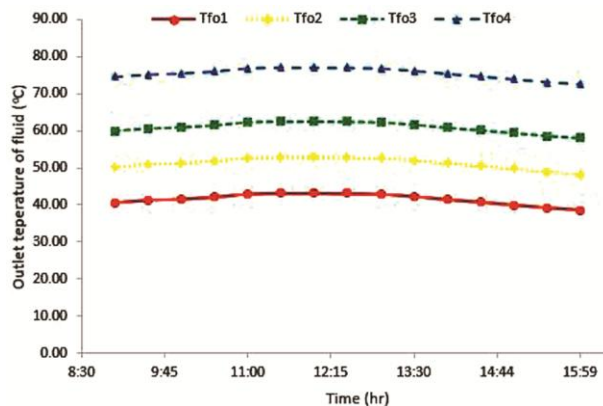


Fig. 4 — Variation of outlet air temperature by varying the kitchen chimney outlet temperature on an hourly basis.

hourly basis are shown in Fig. 3. The predicted results of outlet air, solar cell and absorber plate temperature of the proposed indirect dryer for different kitchen chimney exhaust temperature (37°C, 47°C, 57°C and 72°C) have been shown in Figs (4-6) respectively. From the figures, it has been analysed that outlet air temperature (T_{fo}) increases with an increment of outlet temperature (T_h) of kitchen chimney, as expected. Also, it has been found that, the highest temperature of the solar cell is greater than the absorber plate temperature and absorber plate temperature is greater than the outlet air temperature as expected. Similarly, Eqs. (8 and 9) have been computed and thermal energy and instantaneous thermal efficiency are evaluated for April 2018. The results for different kitchen chimney exhaust temperature (37°C, 47°C, 57°C and 72°C) have been shown in Figs (7 and 8). From the figures, it has been analysed that thermal energy and thermal efficiency increase to their highest value and start decreasing thereafter, as expected. Similarly, Eqs (10 and 11) have been computed for evaluating the electrical

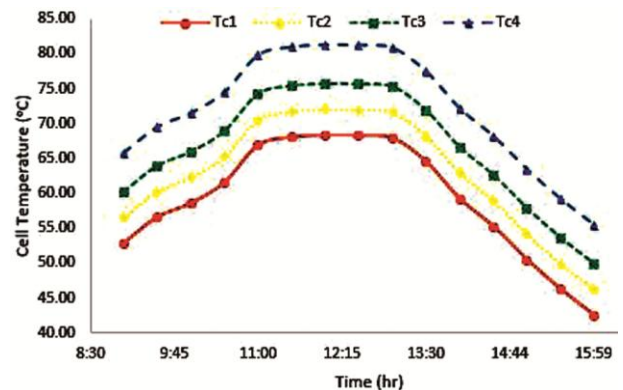


Fig. 5 — Variation of solar cell temperature by varying the kitchen chimney outlet temperature on an hourly basis.

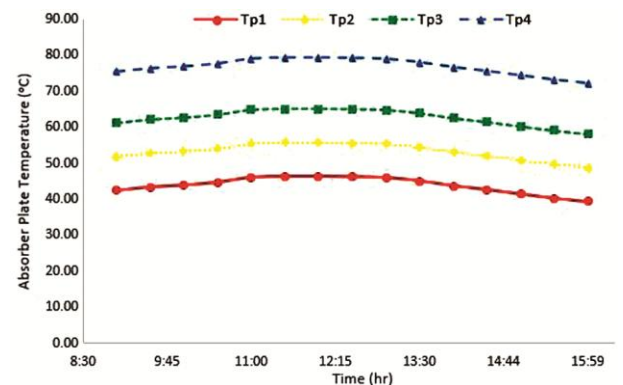


Fig. 6 — Variation of absorber plate temperature by varying kitchen chimney outlet temperature on an hourly basis.

energy and electrical efficiency during April 2018. The results for different kitchen chimney exhaust temperature (37°C, 47°C, 57°C and 72°C)

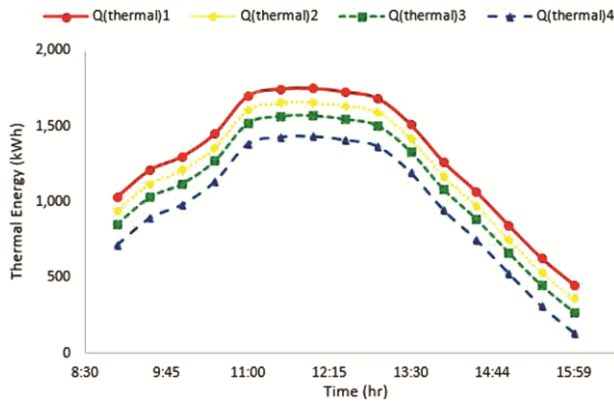


Fig. 7 — Variation of thermal energy with the variation in the kitchen chimney outlet temperature on an hourly basis.

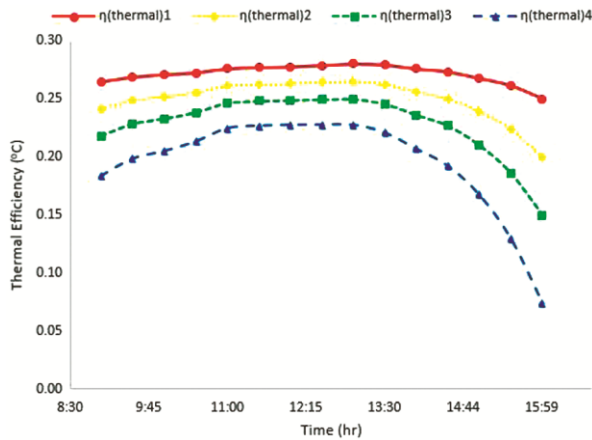


Fig. 8 — Variation of thermal efficiency with the variation in the kitchen chimney outlet temperature on an hourly basis.

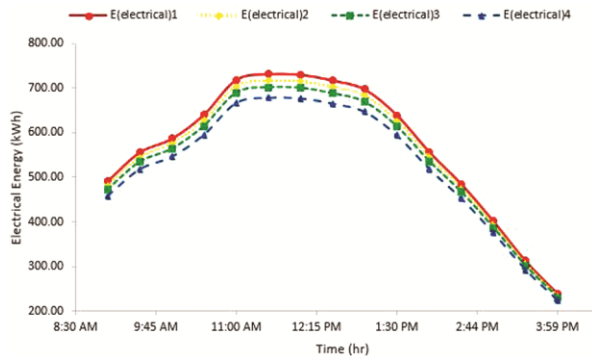


Fig. 9 — Variation of electrical energy on an hourly basis.

have been shown in Figs (9 and 10). Electrical energy increases to its highest value and then starts decreasing with time. Fig. 10 shows that the electrical efficiency decreases with the increment of the cell temperature, and vice versa²³. An hourly gain in the thermal energy, exergy thermal, exergy electrical, exergy destruction have been evaluated by using Eq. (12), and Eqs (14-17). The results obtained through calculation have been shown in Table 2 and the same have been validated using MATLAB by ANN model. Fig. 11 shows the calculated and predicted value obtained by ANN for outlet air temperature with a correlation coefficient of 0.98. Similarly, all other parameters are validated by the ANN method and it has been observed that there is a close agreement between the predicted values and the calculated values.

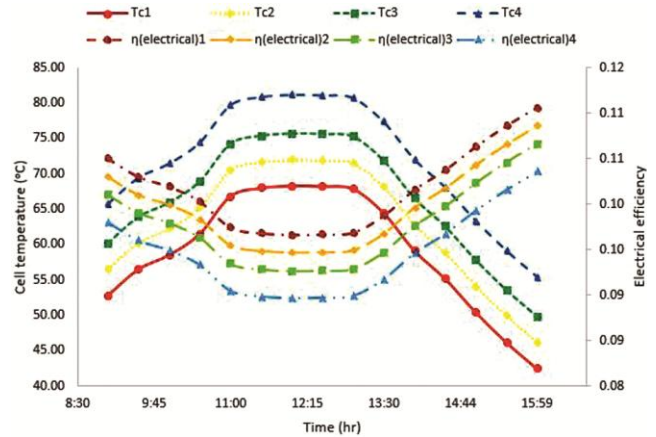


Fig. 10 — Variation of cell temperature and electrical efficiency on an hourly basis with the variation in the kitchen chimney outlet temperature.

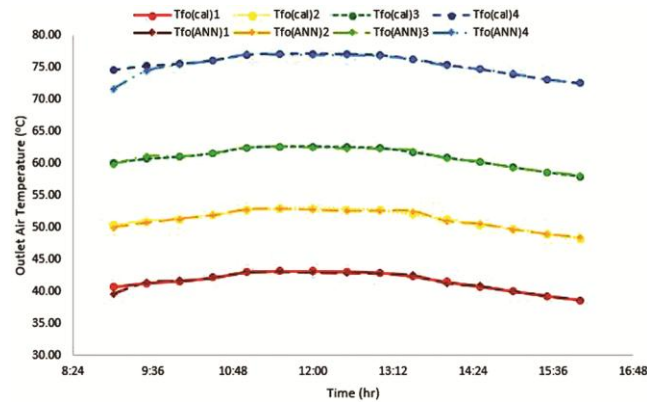


Fig. 11 — Comparison between calculated values and ANN predicted values for outlet air temperature.

Table 2 — Analysis of Energy and Exergy

Time	Energy gain1 (kWh)	Energy gain2 (kWh)	Energy gain3 (kWh)	Energy gain4 (kWh)	Exergy in (kWh)	Exergy out1 (kWh)	Exergy out2 (kWh)	Exergy out3 (kWh)	Exergy out4 (kWh)	Exergy destructed1 (kWh)	Exergy destructed2 (kWh)	Exergy destructed3 (kWh)	Exergy destructed4 (kWh)
9:00	2322.22	2207.51	2092.80	1920.74	3625.18	30.33	36.70	41.17	44.70	3594.85	3588.48	3584.01	3580.48
9:30	2669.35	2550.87	2432.39	2254.67	4182.38	34.55	42.31	48.11	53.47	4147.83	4140.07	4134.28	4128.92
10:00	2841.03	2720.67	2600.30	2419.75	4460.65	36.31	44.82	51.32	57.65	4424.34	4415.83	4409.34	4403.00
10:30	3133.64	3009.97	2886.30	2700.79	4948.54	40.29	49.95	57.52	65.35	4908.24	4898.59	4891.02	4883.19
11:00	3585.08	3456.22	3327.36	3134.07	5713.80	45.04	56.68	66.12	76.54	5668.75	5657.11	5647.68	5637.25
11:30	3666.27	3536.47	3406.66	3211.96	5852.43	45.37	57.43	67.26	78.24	5807.07	5795.00	5785.17	5774.19
12:00	3667.39	3537.59	3407.78	3213.08	5851.70	44.59	56.76	66.68	77.79	5807.11	5794.95	5785.02	5773.92
12:30	3609.62	3480.53	3351.43	3157.79	5745.93	42.43	54.53	64.39	75.41	5703.49	5691.40	5681.54	5670.52
13:00	3512.27	3384.35	3256.44	3064.56	5570.29	39.52	51.42	61.09	71.86	5530.77	5518.87	5509.19	5498.43
13:30	3187.84	3063.70	2939.56	2753.34	5013.26	35.61	46.19	54.63	63.67	4977.64	4967.07	4958.63	4949.59
14:00	2726.29	2607.34	2488.39	2309.96	4248.40	31.34	39.91	46.46	52.87	4217.06	4208.49	4201.94	4195.52
14:30	2340.54	2225.84	2111.13	1939.07	3621.76	26.91	33.95	39.06	43.48	3594.86	3587.82	3582.70	3578.28
15:00	1898.01	1788.02	1678.03	1513.05	2925.85	22.30	27.54	30.95	33.01	2903.55	2898.32	2894.90	2892.84
15:30	1448.47	1343.20	1237.93	1080.02	2229.22	16.93	20.50	22.35	22.22	2212.29	2208.72	2206.87	2207.00
16:00	1077.47	975.97	874.47	722.22	1672.12	12.80	14.94	15.45	13.47	1659.32	1657.18	1656.67	1658.65

4 Conclusion

The following conclusions have been drawn:

From the results,

- (i) It has been concluded that there is an increase of 8°C in drying chamber unit for initial kitchen chimney outlet temperature of 72°C with packing factor of semitransparent module 0.83.
- (ii) All the results has also been validated by using ANN technique on MATLAB.
- (iii) An exhaust fan placed between the PVT air collector and the drying chamber which is operated using electrical energy generated from the PVT air collector.
- (iv) As a results the entire set up is self-sustainable.

References

- 1 Maiti S, Patel P, Vyas K, Eswaran K, & Ghosh PK, *Sol Energy*, 85(11) (2011) 2686.
- 2 El-Sebaei AA, &Shalaby SM, *Energy Convers Manag*, 74 (2013) 109.
- 3 Lingayat A, Chandramohan VP, & Raju VRK, *Energy Procedia*, 109 (2017) 409.
- 4 Hajar E, Rachid T, & Najib BM, *Energy Procedia*, 141(2017) 29.
- 5 El Khadraoui A, Bouadila S, Kooli S, Farhat A, & Guizani A, *J Clean Prod*, 148 (2017) 37.
- 6 Castillo Téllez M, Pilatowsky Figueroa I, Castillo Téllez B, López Vidaña EC, & López Ortiz A, *Sol Energy*, 159 (2018) 898.
- 7 Barnwal P, & Tiwari GN, *Sol Energy*, 82(12) (2008) 1131.
- 8 Nayak S, & Tiwari GN, *Energy Build*, 40(11) (2008) 2015.
- 9 Nayak S, & Tiwari GN, *Energy Build*, 41(8) (2009) 888.
- 10 Kamthania D, Nayak S, &Tiwari GN, *Appl Sol Energy*, 47(3) (2011) 199.
- 11 Agrawal S, & Tiwari GN, *Sol Energy*, 86(9) (2012) 2826.
- 12 Singh S, Agrawal S, & Avasthi D V, *Proc Int Conf Innov Appl Comput Intell Power, Energy Control with Their Impact Humanit CIPECH 2014*, 405.
- 13 Singh S, & Agrawal S, *Energy Convers Manag*, 105 (2015) 763.
- 14 Singh S, Agrawal S, & Gadh R, *Energy Convers Manag*, 105 (2015) 303.
- 15 Nayak S, Kumar A, Singh AK, & Tiwari GN, *Int J Sustain Energy*, 33(2) (2014) 336.
- 16 Gudiño-Ayala D, & Calderón-Topete Á, *Energy Procedia*, 57 (2014) 1642.
- 17 Tiwari S, Tiwari GN, & Al-helal IM, *Sol Energy* 133 (2016) 421.
- 18 Aktas M, Amini A, & Khanlari A, *Sol Energy*, 137 (2016) 500.
- 19 Chandrasekar M, Senthilkumar T, Kumaragurubaran B, & Fernandes JP, *Renew Energy*. Published online 2018.
- 20 Dubey S, Tiwari GN, *Sol Energy*, 82 (2008) 602.
- 21 Huang B, Lin TH, Huang WC, & Sun FS, *Sol Energy* 70(5) (2017).
- 22 Petela R, *Sol Energy*, 86 (2003) 241.
- 23 Evans DL, Simplified method for predicting photovoltaic array output, 27(6) (1981)555.